Electrocardiogram analysis reveals ionic current dysregulation relevant for atrial fibrillation

Albert Dasí[1], Claudia Nagel[2], Axel Loewe[2], Julia Camps[1], Alfonso Bueno-Orovio[1], Blanca Rodriguez[1]

[1]Department of Computer Science, University of Oxford, Oxford, UK
[2]Institute of Biomedical Engineering, Karlsruhe Institute of Technology (KIT), Karlsruhe, Germany

Abstract

Antiarrhythmic drug choice for atrial fibrillation (AF) neglects the individual ionic current profile of the patient, even though it determines drug safety and efficacy. We hypothesize that the electrocardiogram (ECG) might contain information critical for pharmacological treatment personalization. Thus, this study aims to identify the extent of atrial ionic information embedded in the ECG, using multi-scale modeling and simulation.

A dataset of 1,000 simulated ECGs was computed using a population of human-based whole-atria models with 200 individual ionic profiles and 5 different torso-atria orientations. A regression neural network was built to predict key atrial ionic conductances based on P- and T_a-wave biomarkers.

The neural network predicted, with >80% precision, the density of seven ionic currents relevant for AF, namely, ultra-rapid (I_{Kur}), rapid (I_{Kr}), outward transient (I_{to}), inward rectifier K^+ (I_{K1}), L-type Ca^{2+} (I_{CaL}), Na^+/K^+ pump (I_{NaK}) and fast Na^+ (I_{Na}) currents. These ionic densities were identified through the P- (i.e., I_{Na}), T_a- (i.e., I_{K1}, I_{NaK}) or both waves (i.e., I_{Kur}, I_{Kr}, I_{to}, I_{CaL}), providing a non-invasive characterization of the atrial electrophysiology. This could improve patient stratification and cardiac safety and the efficacy of AF pharmacological treatment.

1. Introduction

Pharmacological cardioversion is a fundamental pillar of rhythm-control therapy for atrial fibrillation (AF). Numerous antiarrhythmic drugs have been recommended as first-line treatment in hemodynamically stable patients [1]. Some of these, however, are contraindicated in the context of associated heart disease, given possible cardiotoxicity and proarrhythmia. Interestingly, while proarrhythmic cardiotoxicity has also been strongly associated with the ionic current profile of the patient [2], the latter has so far not been considered for treatment personalization. Inter-patient variability in the ionic current profile is also expected to influence antiarrhythmic drug efficacy [3], so that neglecting it could explain the limited success of AF pharmacological treatment and the high rate of cardiotoxic adverse events.

Albeit ignoring the atrial ionic current profile for drug choice might be due to the inability for its non-invasive characterization, previous studies have observed that analyzing the electrocardiogram (ECG) might reveal atrial conduction properties, the clinical stage of AF [4] or even the percentage of atrial fibrosis [5]. Thus, we hypothesize that the ECG might also contain information on the ionic current properties, which would improve pharmacological treatment personalization, cardiac safety and efficacy. In this regard, modeling and simulations provide a means for generating a well-controlled and rich dataset combining known ionic parameters and associated ECGs, in contrast to clinical recordings. Accordingly, this study aims to assess the prognostic value of the ECG for inferring the atrial ionic current profile, using modeling and simulation.

2. Methods

A dataset of 1,000 ECGs, computed in a population of 200 human-based whole-atria models and considering 5 torso-atria orientations (Figure 1), was used to predict the ionic current profile of the atria. The methodology from single cell to body surface level is described below.

2.1. Population of virtual patient models

An *in-silico* population of atrial cardiomyocyte models was developed as described in [2]. Key conductances and permeabilities of the CRN model [6] were sampled up to ±50% of their control values to capture ionic current variability. Experimental data obtained from human AF and control patients [7] was used for calibration, resulting in 200 atrial cardiomyocyte models (Figure 1C).

Every cardiomyocyte model populated one human-based whole-atria model, by assigning the single-cell properties to the left atrial tissue and scaling them in the remaining atrial regions [8] (Figure 1B-C). Regional heterogeneities in conduction velocity and anisotropy ratio were likewise considered [8], setting the longitudinal conduction velocity in the bulk tissue to 80 cm/s.

Sinus rhythm was simulated in the virtual cohort of 200 whole-atria models for 5 beats, starting with the steady-state conditions at single cell. The 3D monodomain equation of the transmembrane voltage was solved using the MonoAlg3D program [9].

2.2. Electrocardiogram analysis

Standard 12-lead and extended 15-lead [4] ECGs were computed as in [10] during the sixth sinus rhythm beat. The atrial geometry was rotated ±30º around the y- and z-axis, resulting in 5 ECG calculations per whole-atria model (Figure 1A). Six biomarkers, namely duration, amplitude, area, Shannon entropy, sample entropy and complexity [4], were calculated lead-wise from the P- and T_a-wave. Three additional biomarkers were obtained for the P-wave: actual duration (as the last activation time extracted from the simulations), dispersion and V1 terminal force.

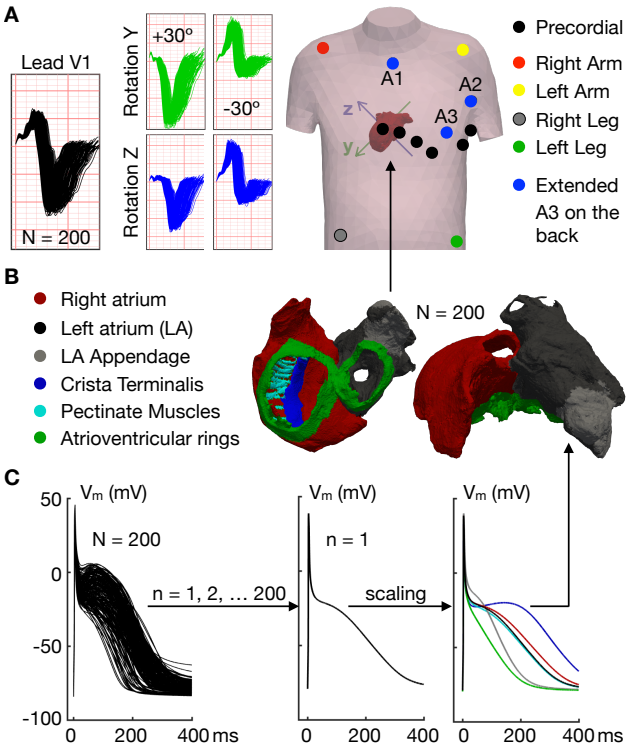

Figure 1. Simulated 15-lead ECG in the cohort of virtual patient models. Colors for the action potentials (V_m) in C) like in B).

2.3. Regression with neural networks

A complete dataset was generated considering the P- and T_a-wave biomarkers from 1,000 ECGs (ECG for 200 whole-atria models with 5 torso-atria orientations). The dataset was partitioned into four sub-datasets to compare the prognostic value of P- vs. T_a-wave and 12- vs. 15-lead ECG for predicting the ionic current densities of the atria.

A regression neural network was built as in [5], randomly allocating 70-15-15% of the data for training, validation and testing, respectively. The performance was assessed through the root mean squared error (RMSE). Furthermore, a multi-class classification problem was set by grouping the ionic current distribution into low ([–50, –20] %), middle ((–20, +20) %) or high ([+20, +50] %) ionic density, allowing evaluation of precision and recall.

3. Results and discussion

3.1. Fast Na^+ and inward rectifier K^+ currents dictate P- and T_a-wave duration, respectively

Figure 2 illustrates the influence of the fast Na^+ (I_{Na}) and inward rectifier K^+ (I_{K1}) currents on the P- and T_a-wave and the neural network prediction of their ionic densities.

I_{Na} and I_{K1} were markedly associated with the P- and T_a-wave duration, respectively, with their up-regulation causing a prominent wave shortening (Figure 2, top). Accordingly, the neural network predicted their ionic current density with an error below 5% (Figure 2, bottom).

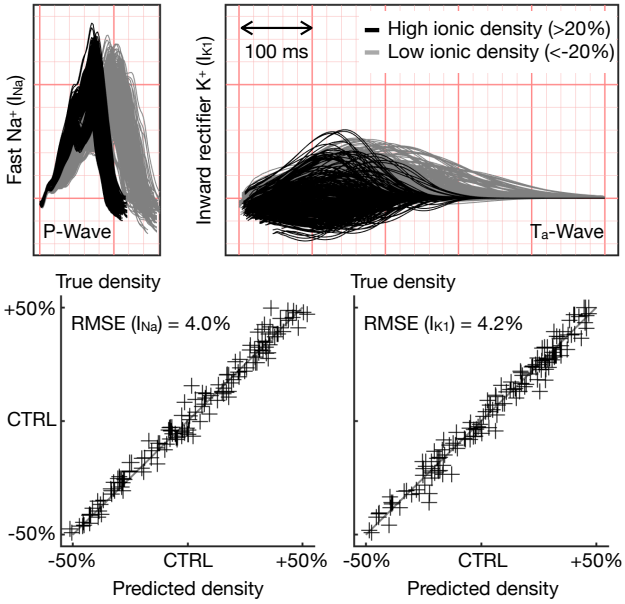

Figure 2. Effects of I_{Na} and I_{K1} on the P- and T_a-wave (lead V6). Performance, root mean squared error (RMSE), for the prediction of I_{Na} and I_{K1} density. CTRL: Control ionic current density.

3.2. Rapid rectifier K^+ and Na^+/K^+ pump currents determine the amplitude and complexity of the T_a-wave

Figure 3 illustrates the prediction of the rapid rectifier K^+ (I_{Kr}), transient outward K^+ (I_{to}) and Na^+/K^+ pump (I_{NaK}) densities. Average errors below 12% were obtained for all three currents, as they were key modulators of the T_a-wave.

T_a-wave amplitude and area showed a proportional

relationship with I_{NaK}, with high I_{NaK} density causing large T_a-waves in the precordial leads (Figure 3, top). The amplitude was to a lower extent associated with I_{Kr}, although I_{Kr} primarily influenced the signal complexity. As such, elevated I_{Kr} yielded less complex T_a-waves, (i.e., characterized by fewer local peaks), potentially due to a more homogeneous cellular repolarization.

I_{to} influenced both P- and T_a-wave biomarkers. While high I_{to} density increased T_a-wave sample entropy, it reduced P-wave Shannon entropy. Moreover, elevated I_{to} decreased P-wave amplitude and area, due to a reduction in the action potential amplitude. However, P-wave biomarkers showed a predominant relationship with I_{Na}.

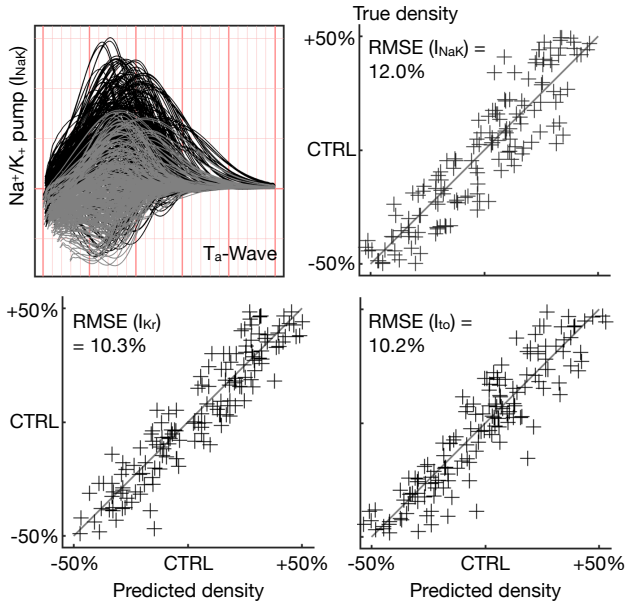

Figure 3. Effects of I_{NaK} on the T_a-wave (lead V6). Prediction of I_{NaK}, I_{Kr} and I_{to} density. Colors and abbreviations as in Figure 2.

3.3. Electrocardiogram metrics identify ionic current dysregulation relevant to AF

Figure 4 illustrates precision, recall and confusion matrix for the classification of the ultra-rapid rectifier K^+ (I_{Kur}), L-type Ca^{2+} (I_{CaL}), I_{Kr}, I_{K1}, I_{NaK} and I_{Na} density, using P- and T_a-wave biomarkers from the 12-lead ECG.

As anticipated in Figure 2, very high precision and recall were obtained for I_{Na} classification. An accurate estimation of I_{Na} density could be crucial for AF treatment with class Ic agents, such as flecainide or propafenone. These drugs are the preferred choice for AF cardioversion, only contraindicated in structurally severe or ischemic heart disease [1]. However, previous *in-silico* studies have shown that flecainide caused depolarization abnormalities in cells with low I_{Na} density [2].

Similarly, repolarization abnormalities, such as early and delayed afterdepolarizations [11], and increased automaticity [12] have been documented for I_{NaK} and I_{K1} inhibition. Paradoxically, increased I_{K1} and I_{NaK} are a hallmark of AF, so that blocking either current represents a well-established approach for AF termination [11,12]. Accordingly, an accurate, non-invasive characterization of I_{K1} and I_{NaK} density (as illustrated in Figure 4) could help planning safer and more efficacious AF pharmacological treatments with I_{K1} and I_{NaK} inhibitors.

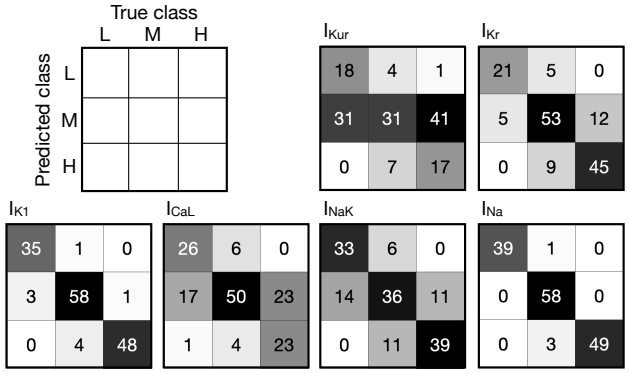

	High Density (>20%)		Low Density (<-20%)	
	Precision	Recall	Precision	Recall
I_{Kur}	0.71	0.29	0.78	0.37
I_{Kr}	0.83	0.79	0.81	0.81
I_{K1}	0.92	0.98	0.97	0.92
I_{CaL}	0.82	0.50	0.81	0.59
I_{NaK}	0.78	0.78	0.85	0.70
I_{Na}	0.94	1.00	0.97	1.00

Figure 4. Confusion matrix, precision and recall for the multi-class classification of I_{Kur}, I_{Kr}, I_{K1}, I_{CaL}, I_{NaK} and I_{Na} density. Abbreviations: L-M-H: Low, middle and high density.

Multiple class III agents, such as amiodarone, dronedarone, ibutilide and vernakalant, block I_{Kr}, I_{Kur} or both. Pharmacological I_{Kr} inhibitors are used with caution, given potential QT prolongation and risk for polymorphic ventricular tachycardia. Accordingly, knowing I_{Kr} density (Figure 4: precision and recall around 80%,), could reduce the number of proarrhythmic adverse events.

Still, the lack of safety associated with I_{Kr} blockers made AF pharmacological treatment to consider atrial-selective targets, such as I_{Kur}. I_{Kur} inhibition, however, has shown limited efficacy in clinical trials, potentially due to I_{Kur} down-regulation in AF patients [13]. Thus, estimating I_{Kur} density could enable a better use of I_{Kur} inhibitors, such as vernakalant. In this sense, a high precision was obtained for I_{Kur} classification, despite a low recall (Figure 4).

Similar results were obtained for I_{CaL} classification. Estimating I_{CaL} down-regulation with high precision (Figure 4) could help inferring about the stage of AF electrophysiological remodeling. Moreover, since baseline I_{Na} and I_{CaL} densities have been suggested to play an important role on the efficacy of blocking the inward currents [14], estimating them could be crucial for the selection of class Ic and class IV antiarrhythmic drugs.

3.4. Both P- and T_a-wave are needed for characterizing the atrial ionic profile

The RMSE differed less than 1% when the neural network was trained with 12- or 15-lead ECG, with the latter adding marginal gain. However, the prediction of all ionic densities required biomarkers from the P- (i.e., I_{Na}) T_a- (i.e., I_{K1}, I_{NaK}), or both waves (i.e., I_{to}, I_{Kr}, I_{Kur}, I_{CaL}). This poses the question as to whether the T_a-wave could be obtained through an improved electrode configuration [15], so that adenosine administration could be avoided.

4. Conclusion

The ionic current profile of the atria has been non-invasively characterized in a virtual cohort of patient models, showing that ionic current dysregulations critical for AF can be identified through the analysis of the P- and T_a-wave. All simulations were conducted using the same atrial geometry and electrode positions. However, the size and shape of the atria, structural heterogeneities (i.e., atrial fibrosis) and the distance of the electrodes with respect to the heart are known factors that influence the duration and amplitude of ECG waves [5].

Therefore, although further work is needed to take these parameters into account, the non-invasive characterization of the atrial ionic profile could improve patient stratification, cardiac safety and the efficacy of AF pharmacological treatment.

Acknowledgments

AD is funded by the PersonalizeAF project, European Union's Horizon 2020 research and innovation programme under the Marie Sklodowska-Curie grant agreement 860974. The authors acknowledge further support from British Heart Foundation (FS/17/22/32644), Wellcome Trust (214290/Z/18/Z), NC3Rs (NC/P001076/1), the CompBioMed Centre of Excellence in Computational Biomedicine (European Union's Horizon 2020, grant agreements 675451, 823712), and PRACE for awarding us access to Piz Daint at the Swiss National Supercomputing Centre, Switzerland (ICEI-PRACE grant icp013).

References

[1] G. Hindricks *et al.*, "2020 ESC Guidelines for the diagnosis and management of atrial fibrillation developed in collaboration with the European Association for Cardio-Thoracic Surgery (EACTS)," *Eur. Heart J.*, vol. 42, no. 5, pp. 373–498, 2021.

[2] E. Passini *et al.*, "Human in silico drug trials demonstrate higher accuracy than animal models in predicting clinical pro-arrhythmic cardiotoxicity," *Front. Physiol.*, vol. 8, no. SEP, pp. 1–15, 2017.

[3] A. Capucci, L. Cipolletta, F. Guerra, and I. Giannini, "Emerging pharmacotherapies for the treatment of atrial fibrillation," *Expert Opin. Emerg. Drugs*, vol. 23, no. 1, pp. 25–36, 2018.

[4] M. D. Zink *et al.*, "Extended ECG Improves Classification of Paroxysmal and Persistent Atrial Fibrillation Based on P- and f-Waves," *Front. Physiol.*, vol. 13, no. March, pp. 1–12, 2022.

[5] C. Nagel, G. Luongo, L. Azzolin, S. Schuler, O. Dössel, and A. Loewe, "Non-invasive and quantitative estimation of left atrial fibrosis based on p waves of the 12-lead ecg—a large-scale computational study covering anatomical variability," *J. Clin. Med.*, vol. 10, no. 8, p. 1797, 2021.

[6] M. Courtemanche, R. J. Ramirez, and S. Nattel, "Ionic mechanisms underlying human atrial action potential properties: Insights from a mathematical model," *Am. J. Physiol. - Hear. Circ. Physiol.*, vol. 275, no. 1 44-1, 1998.

[7] C. Sánchez *et al.*, "Inter-subject variability in human atrial action potential in sinus rhythm versus chronic atrial fibrillation," *PLoS One*, vol. 9, no. 8, 2014.

[8] C. Sánchez, A. Bueno-Orovio, E. Pueyo, and B. Rodríguez, "Atrial fibrillation dynamics and ionic block effects in six Heterogeneous human 3D virtual atria with distinct repolarization dynamics," *Front. Bioeng. Biotechnol.*, vol. 5, no. MAY, pp. 1–13, 2017.

[9] R. Sachetto Oliveira, B. Martins Rocha, D. Burgarelli, W. Meira, C. Constantinides, and R. Weber dos Santos, "Performance evaluation of GPU parallelization, space-time adaptive algorithms, and their combination for simulating cardiac electrophysiology," *Int. j. numer. method. biomed. eng.*, vol. 34, no. 2, pp. 1–17, 2018.

[10] K. Gima and Y. Rudy, "Ionic current basis of electrocardiographic waveforms: A model study," *Circ. Res.*, vol. 90, no. 8, pp. 889–896, 2002.

[11] A. Bueno-Orovio, C. Sánchez, E. Pueyo, and B. Rodriguez, "Na/K pump regulation of cardiac repolarization: Insights from a systems biology approach," *Pflugers Arch. Eur. J. Physiol.*, vol. 466, no. 2, pp. 183–193, 2014.

[12] D. Filgueiras-Rama *et al.*, "Chloroquine terminates stretch-induced atrial fibrillation more effectively than flecainide in the sheep heart," *Circ. Arrhythmia Electrophysiol.*, vol. 5, no. 3, pp. 561–570, 2012.

[13] J. Heijman, S. H. Hohnloser, and A. John Camm, "Antiarrhythmic drugs for atrial fibrillation: Lessons from the past and opportunities for the future," *Europace*, vol. 23, pp. II14–II22, 2021.

[14] A. Liberos *et al.*, "Balance between sodium and calcium currents underlying chronic atrial fibrillation termination: An in silico intersubject variability study," *Hear. Rhythm*, vol. 13, no. 12, pp. 2358–2365, 2016.

[15] S. Jayaraman, U. Gandhi, V. Sangareddi, U. Mangalanathan, and R. M. Shanmugam, "Unmasking of atrial repolarization waves using a simple modified limb lead system," *Anatol. J. Cardiol.*, vol. 15, no. 8, pp. 605–610, 2015.

Address for correspondence:

Albert Dasí.
Department of Computer Science, University of Oxford,
Wolfson Building, Parks Road, Oxford, OX1 3QD, UK.
albert.dasiimartinez@cs.ox.ac.uk